On the Detection Probability of Parallel Code Phase Search Algorithms in GPS Receivers

Bernhard C. Geiger, Michael Soudan, Christian Vogel
Signal Processing and Speech Communication Laboratory
Graz University of Technology, Austria
{geiger,msoudan,vogel}@tugraz.at

***Abstract*—The first stage of the signal processing chain in a Global Positioning System (GPS) receiver is the acquisition, which provides for a desired satellite coarse code phase and Doppler frequency estimates to subsequent stages. Thus, acquisition is a two-dimensional search, implemented as demodulation and non-coherent correlation. For a certain Doppler estimate, software-defined GPS receivers typically compute the correlation for all time lags in parallel.**

One way to detect the presence of a signal is by comparing the ratio between the largest and the second largest correlation peak against a threshold. For this type of receivers, the detection and false alarm probabilities are derived. Interestingly, the false alarm probability is independent of the noise power spectral density, which allows a fixed threshold setting. The analytic results are verified by a series of simulations.

I. Introduction

In conventional Global Positioning System (GPS) receivers a particular satellite is acquired by comparing the correlation coefficients between the received signal and a local code signal against a threshold. Every satellite is transmitting a particular pseudo-random noise (PRN) code, which is available at the receiver as a local replica. This local code signal differs from the received code signal by a time lag and a Doppler shift, and a two-dimensional search is required for each satellite.

The advent of software-defined GPS receivers facilitated the use of the parallel code phase search, which computes the circular correlation function for a given Doppler estimate for all time lags in a single step. This feature is especially interesting when taking current GPS modernization efforts into consideration. New civil signals consist of PRN codes of a much longer code period that make a serial search too time consuming. The parallel code phase search can be efficiently implemented using the fast Fourier transform (FFT), which can be used to perform circular correlations by means of multiplying spectra in the frequency domain.

One way to determine if a particular code is present is to relate the largest correlation peak to the second largest one for all possible Doppler frequencies. The ratio between the largest and second largest correlation peak was introduced as a confidence measure for acquisition in [1]. In [2], this measure was first used to perform acquisition, motivated by the assumption that the false alarm probability is independent of the threshold. Although its performance has not been proven to be superior compared to standard confidence measures, the method was patented [3] and adopted by many researchers, e.g. [4].

For non-coherent acquisition methods, which take the squared magnitude of the correlation function as a decision metric to cope with unknown phase shifts of the carrier and possible data modulation, the computation of the receiver operating characteristics is a well-investigated field of research. The literature gives expressions for single elements (cells) of the correlation function [5], a serial search with threshold comparison [6], [7], a maximum search [8], [9] and combinations thereof [10]. In [11], a comparison of the above-mentioned techniques is provided for an L1 GPS receiver. Detection probabilities for an L5 GPS receiver with different algorithms combining data and pilot signals are considered in [12], from which the comprehensive signal model was largely adopted in this work. Still, expressions for the false alarm and the detection probabilities in a scenario where the ratio between the two largest correlation peaks is compared against a threshold can not be found in the literature. It is the purpose of this work to elaborate this acquisition method and derive the receiver operating characteristics for a given Doppler estimate. Moreover, it will be shown analytically that such a method makes the false alarm probability independent of the noise power spectral density (PSD) and thus can use a fixed threshold to obtain a constant false alarm rate. Although the derivations are performed for a GPS signal model, the results can be applied to other CDMA systems as well.

The remainder of this paper is organized as follows: In Section II the signal model is established, while Section III gives a detailed analysis of the acquisition process. Sections IV, V, and VI derive expressions for the false alarm and detection probabilities for different signal strengths. A series of simulations verifies the obtained results in Section VII.

II. Signal Model

After front-end filtering, downconversion to the intermediate frequency (IF) and A/D conversion the signal received from a single satellite can be represented as

$$r_{IF}[n] = \sqrt{2C}\, y[n] \cos\Big[(\theta_{IF} + \theta_D)\, n - \vartheta\Big] + \eta[n] \quad (1)$$

where $\theta_{IF} = \frac{2\pi f_{IF}}{f_s}$ and $\theta_D = \frac{2\pi f_D}{f_s}$ are the sampled equivalents of the intermediate and Doppler frequencies f_{IF} and f_D, respectively, and ϑ is a phase shift introduced by

978-1-4244-8016-6/10/$26.00 ©2010 IEEE

transmission and downconversion to IF. The white Gaussian noise signal $\eta[n]$ has a variance $\sigma_\eta^2 = \frac{N_0 f_s}{2}$ with $\frac{N_o}{2}$ being the two-sided noise PSD and f_s the sampling frequency of the A/D converter. The spreading code sequence with power C is denoted by

$$y[n] = d[n]c[n] \tag{2}$$

where $d[n]$ is the data message. The PRN code $c[n]$ is either the L1 C/A code or a time-multiplexing of the L2 CM and CL codes [5]. The number of chips per code is N_C, so with a chip period T_C one code period is $T_{per} = N_C T_C$. Acquisition is either performed using the L1 C/A code or the L2 CM code, which has to be spread with zeros prior to correlation to cope with time multiplexing [13]. The L1 C/A code consists of 1023 chips and has a period of $T_{per} = 1$ ms, whereas the L2 CM code has 10230 chips (20460 after zero spreading) and a period of 20 ms. The longer L2 CL code, that is constituted by 767250 chips and a period of 1.5 s, is impractical for acquisition and will not be considered [13]. To simplify the derivation, it is assumed that no data is modulated on the PRN codes, i.e., $d[n] = 1$. While this assumption is justified for the L1 C/A codes[1], in an acquisition system for L2 CM codes the effects of bit transitions can be mitigated using non-coherent integration [14] or aided acquisition [1].

According to [5], [14] the cross-correlation power levels between different L1 C/A codes and between the multiplexed L2 CM+CL code and the L2 CM code with interspersed zeros are below -21 dB and -27 dB, respectively, which justifies the assumption of the single satellite case. Still, side lobe and cross-correlation levels may exceed the noise floor and will be considered in the following analyses.

III. Acquisition process

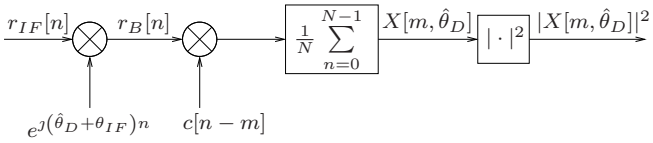

Fig. 1. Acquisition of a signal with unknown Doppler frequency and code phase.

In the acquisition process (see Fig. 1), the received signal $r_{IF}[n]$ is first demodulated using an expected Doppler frequency $\hat{\theta}_D$. The obtained signal $r_B[n] = r_{IF}[n]e^{\jmath(\hat{\theta}_D+\theta_{IF})n}$ is thus described by

$$r_B[n] = \sqrt{\frac{C}{2}}y[n]\left(e^{\jmath(2\theta_{IF}+\Sigma\theta_D)n-\jmath\vartheta} + e^{\jmath\Delta\theta_D n+\jmath\vartheta}\right) + \tilde{\eta}[n] \tag{3}$$

with $\Delta\theta_D = \hat{\theta}_D - \theta_D$ and $\Sigma\theta_D = \hat{\theta}_D + \theta_D$. The noise signal $\tilde{\eta}[n]$ is a zero-mean circular symmetric complex Gaussian (ZMCSCG) signal with the variances of the real and imaginary parts equal to $\frac{\sigma_\eta^2}{2}$. After demodulation the signal is circularly correlated with the spreading code using an expected code phase m. Thus, the decision metric $X[m,\hat{\theta}_D]$ is

$$X[m,\hat{\theta}_D] = \frac{1}{N}\sum_{n=0}^{N-1} r_B[n]c[n-m] \tag{4}$$

where $c[n-m]$ is the PRN code $c[n]$ with a period of $N = \frac{T_{per}}{T_s}$ samples circularly shifted by m. Through the filter operation in (4), the high-frequency term $e^{\jmath(2\theta_{IF}+\Sigma\theta_D)n-\jmath\vartheta}$ can be neglected and the correlation of $y[n]$ and the code can be represented by the circular correlation function $R_{y,c}[m]$. The summation over the low-frequency term can be expressed by a finite sum, which for small Doppler frequencies approximates to

$$\begin{aligned}\frac{1}{N}\sum_{n=0}^{N-1} e^{\jmath\Delta\theta_D n} &= e^{\jmath\Delta\theta_D\frac{N-1}{2}}\frac{\sin\left(\frac{\Delta\theta_D}{2}N\right)}{N\sin\left(\frac{\Delta\theta_D}{2}\right)} \\ &\approx e^{\jmath\Delta\theta_D\frac{N-1}{2}}\operatorname{sinc}\left(\frac{\Delta\theta_D}{2\pi}N\right).\end{aligned} \tag{5}$$

Following the reasoning in [15], the influences of time lags and Doppler frequencies can be separated, which is supported by extensive simulations showing that the error resulting from this approximation is well below -21 dB and thus is masked by maximum side lobe levels [5]. Having further that $\Delta\theta_D = 2\pi\frac{\Delta f_D}{f_s} = 2\pi\Delta f_D\frac{T_{per}}{N}$ we thus obtain for the decision metric

$$\begin{aligned}&X[m,\hat{\theta}_D] = \\ &\quad e^{\jmath\Delta\theta_D\frac{N-1}{2}+\jmath\vartheta}\operatorname{sinc}\left(\Delta f_D T_{per}\right)\sqrt{\frac{C}{2}}R_{y,c}[m] + n[m].\end{aligned} \tag{6}$$

The noise signal $n[m]$ is the average of N independent ZMCSCG samples, thus the variances of the real and imaginary parts reduce to

$$\frac{\sigma_n^2}{2} = \frac{\sigma_\eta^2}{2N} = \frac{N_0 f_s}{4N} = \frac{N_0}{4T_{per}}. \tag{7}$$

When the spreading code $c[n]$ is upsampled to the sampling rate f_s, the noise samples $n[m]$ in the decision metric are not necessarily independent anymore. To guarantee independency, we will assume for the remainder of this work that the sampling period T_s at which correlation is performed is in the order of the chip period T_C. This assumption is justified by the fact that numerous references (e.g., [16], [17]) pursue approaches to reduce the number of samples for correlation by means of coherent integration.

The decision is finally based on the squared magnitude of the decision metric $X[m,\hat{\theta}_D]$, which follows a non-central χ^2-distribution with two degrees of freedom and with the non-centrality parameter L given by

$$\begin{aligned}L &= \frac{\mathrm{E}\left\{\Re\{X[m,\hat{\theta}_D]\}\right\}^2}{\frac{\sigma_n^2}{2}} + \frac{\mathrm{E}\left\{\Im\{X[m,\hat{\theta}_D]\}\right\}^2}{\frac{\sigma_n^2}{2}} \\ &= 2T_{per}\frac{C}{N_0}\operatorname{sinc}^2\left(\Delta f_D T_{per}\right)R_{y,c}^2[m]\end{aligned} \tag{8}$$

[1] In [4] for example, acquisition is performed twice for two consecutive C/A code periods. By taking the result with the stronger correlation peak, it can be guaranteed that no bit transition occurred within the considered integration period.

where the squared means of the real and imaginary parts have been normalized by their variances.

Software-defined GPS receivers often exploit the properties of the FFT to compute the decision metric for one domain (i.e. code or frequency) in a single step. One of the most widespread algorithms is the parallel code phase search algorithm, which implements the circular correlation in (4) as a multiplication in the frequency domain. By computing the inverse FFT, the circular correlation function is obtained for all lags m simultaneously. This procedure has to be repeated for all possible Doppler frequencies, as the sinc kernel in (8) suggests.

The proposed satellite acquisition technique for a fixed code corresponding to a specific satellite operates as follows:

1) Compute the decision metric $|X[m,\hat{\theta}_D]|^2$ for an estimated Doppler frequency $\hat{\theta}_D$.
2) Find the maximum $m_{\max} = \arg\max_m \left\{|X[m,\hat{\theta}_D]|^2\right\}$.
3) From the decision metric, exclude N_{excl} samples surrounding the maximum $m_{\max}$, where N_{excl} is the width of the main lobe of the code's autocorrelation function $R_{c,c}[m]$.
4) Find the second maximum $m_{2\text{ndmax}} = \arg\max_{m\neq m_{\max}\pm N_{\text{excl}}} \left\{|X[m,\hat{\theta}_D]|^2\right\}$ from the remaining portion of the decision metric $|X[m,\hat{\theta}_D]|^2$
5) If $\frac{|X[m_{\max},\hat{\theta}_D]|^2}{|X[m_{2\text{ndmax}},\hat{\theta}_D]|^2} > \beta$ the satellite is acquired successfully, otherwise the procedure is repeated with the next $\hat{\theta}_D$ until the whole Doppler range is searched.

Although this method is widely adopted in software-defined GPS receivers (see for example [4]), a derivation of the detection and false alarm probabilities is still pending.

IV. False Alarm Probability

Unless the desired code is contained in the input signal, the correlation function $R_{y,c}[m] \approx 0$ and the distribution of the decision metric $|X[m,\hat{\theta}_D]|^2$ changes from a non-central to a central χ^2-distribution with two degrees of freedom. To simplify the argument, it is assumed that the maximum found in the remaining portion of the decision metric $|X[m,\hat{\theta}_D]|^2$ is identical to the second maximum of the whole decision metric. This assumption is justified by the fact that the exclusion range N_{excl} is related to the support of the main lobe of the autocorrelation function $R_{c,c}[m]$ of the spreading code. For the civil codes on L1 and L2, the exclusion range is $2N_{\text{excl}} = 2\left(\frac{T_C}{T_s} - 1\right) \ll N$ and the reduced search range is $N_{\text{r}} = N - 2N_{\text{excl}} - 1 \approx N$. According to this, the equation for the false alarm probability simplifies to

$$P_{fa}(\beta) = \mathrm{P}\left(\frac{\max_m \left\{|X[m,\hat{\theta}_D]|^2\right\}}{\max_{m\neq m_{\max}} \left\{|X[m,\hat{\theta}_D]|^2\right\}} > \beta\right). \quad (9)$$

To maintain mathematical rigor, the outcome of this derivation will be referred to as a lower bound on the false alarm probability. This is intuitively understood since by increasing the number of samples over which the search is performed the expected value of the second maximum increases. Correspondingly, the ratio between the first and second maximum reduces, which leads to a decreased false alarm probability. The bound is tighter for spreading codes of greater length N_C. Moreover, the bound is tight for $N = N_C$ since then $T_C = T_s$ and $N_{\text{excl}} = 0$.

Let $X_{(N)} = \max_m \left\{|X[m,\hat{\theta}_D]|^2\right\}$ denote a random variable (RV) taking the value of the maximum of the complete decision metric and let $X_{(N-1)} = \max_{m\neq m_{\max}} \left\{|X[m,\hat{\theta}_D]|^2\right\}$ denote a RV taking the value of the second maximum. The false alarm probability is

$$P_{fa}(\beta) = \mathrm{P}\left(\frac{X_{(N)}}{X_{(N-1)}} > \beta\right) = \mathrm{P}\left(X_{(N)} > \beta X_{(N-1)}\right) \quad (10)$$

where $\beta \geq 1$. According to [18, pp. 186], this can be computed with the formula

$$P_{fa}(\beta) = \int_0^\infty \int_{\beta x}^\infty f_{(N-1,N)}(x,y)\,dy\,dx \quad (11)$$

where $f_{(N-1,N)}(x,y)$ is the joint probability density function (PDF) of the first and second maximum. From the theory of order statistics [19, pp. 12], this is equivalent to

$$P_{fa}(\beta) = \int_0^\infty \int_{\beta x}^\infty (N^2 - N) f_X(x) f_X(y) F_X^{N-2}(x)\,dy\,dx. \quad (12)$$

Knowing that the distribution of the samples is a central χ^2-distribution with two degrees of freedom, we get the PDF $f_X(x) = \frac{1}{2}e^{-\frac{x}{2}}$ and the cumulative density function (CDF) $F_X(x) = 1 - e^{-\frac{x}{2}}$. Now we can calculate the false alarm probability, i.e.

$$\begin{aligned} P_{fa}(\beta) &= \frac{N^2-N}{4} \int_0^\infty \int_{\beta x}^\infty e^{-\frac{x+y}{2}} \left(1 - e^{-\frac{x}{2}}\right)^{N-2} dy\,dx \\ &= \frac{N^2-N}{2} \int_0^\infty e^{-\frac{x+\beta x}{2}} \left(1 - e^{-\frac{x}{2}}\right)^{N-2} dx. \end{aligned} \quad (13)$$

After substituting $u = e^{-\frac{x}{2}}$ we get

$$\begin{aligned} P_{fa}(\beta) &= (N^2-N) \int_0^1 u^\beta (1-u)^{N-2}\,du \\ &= (N^2-N)\mathrm{B}(N-1, 1+\beta) \end{aligned} \quad (14)$$

where $\mathrm{B}(\cdot,\cdot)$ is the Beta function [20, pp. 258]. From (14) we conclude that in the case no signal is present, the false alarm probability only depends on the value of the threshold β and the length N of the correlation function. Interestingly, by taking the ratio between two correlation peaks, the false alarm probability is independent of the noise PSD N_0. Furthermore, the false alarm probability is independent of the satellite's signal power as long as cross-correlations with orthogonal codes are well below the noise floor.

V. Detection Probability for Weak Signals

This section accounts for cases where the desired signal is weak, so that the correlation main lobe exceeds the noise

floor but the side lobes do not. The probability of detection is calculated as the probability that the signal sample exceeds the largest noise sample by a factor β. Here, on the other hand, the largest and second largest peaks are not identically distributed – while the largest peak results from the presence of a signal, the second largest peak is assumed to stem from the noise-only portion of the correlation function. This assumption underestimates the value of the second largest peak and provides an upper bound on the derived probabilty.

The largest noise sample, $X_{(N_\mathrm{r})}$, is the maximum of a set of N_r centrally χ^2-distributed RVs, while the signal sample, Y, follows a non-central χ^2-distribution with parameter L according to (8). Since these RVs are independent, it is possible to write the joint PDF as a factor of the separate PDFs:

$$\begin{aligned} P_d(\beta) &= \mathrm{P}\left(\frac{Y}{X_{(N_\mathrm{r})}} > \beta\right) = \mathrm{P}\left(X_{(N_\mathrm{r})} < \frac{Y}{\beta}\right) \\ &= \int_0^\infty \int_0^{\frac{y}{\beta}} f_Y(y) f_{(N_\mathrm{r})}(x) dx dy \\ &= \int_0^\infty f_Y(y) F_{(N_\mathrm{r})}\left(\frac{y}{\beta}\right) dy \end{aligned} \tag{15}$$

$F_{(N_\mathrm{r})}(x)$ is the CDF of the maximum of a set of N_r samples from a centrally χ^2-distributed RV, for which we have [18, pp. 246]

$$F_{(N_\mathrm{r})} = F_X^{N_\mathrm{r}}(x) = \left(1 - e^{-\frac{x}{2}}\right)^{N_\mathrm{r}}. \tag{16}$$

For the non-central χ^2-distribution with two degrees of freedom the PDF is given as

$$f_Y(y) = \frac{1}{2} e^{-\frac{y+L}{2}} \sum_{q=0}^{\infty} \frac{(Ly)^q}{4^q \left(q!\right)^2}. \tag{17}$$

Inserting (16) and (17) into (15) and rearranging summation and integration yields

$$P_d(\beta) = \frac{e^{-\frac{L}{2}}}{2} \sum_{q=0}^{\infty} \left[\frac{L^q}{4^q \left(q!\right)^2} \int_0^\infty y^q e^{-\frac{y}{2}} \left(1 - e^{-\frac{y}{2\beta}}\right)^{N_\mathrm{r}} dy \right]. \tag{18}$$

The latter equation can be expanded into a binomial series:

$$\begin{aligned} P_d(\beta) &= \frac{e^{-\frac{L}{2}}}{2} \sum_{q=0}^{\infty} \left[\frac{L^q}{4^q \left(q!\right)^2} \right. \\ &\quad \left. \times \sum_{k=0}^{N_\mathrm{r}} \left[(-1)^k \binom{N_\mathrm{r}}{k} \int_0^\infty y^q e^{-\frac{y}{2}} e^{-\frac{yk}{2\beta}} dy \right] \right] \\ &= e^{-\frac{L}{2}} \sum_{q=0}^{\infty} \left[\frac{L^q}{2^q q!} \right. \\ &\quad \left. \times \, {}_{q+2}F_{q+1}\left([-N_\mathrm{r}, \beta \mathbf{1}_{q+1}]; (\beta+1)\mathbf{1}_{q+1}; 1\right) \right]. \end{aligned} \tag{19}$$

where ${}_pF_q\left([a_1, \ldots, a_p]; [b_1, \ldots, b_q]; c\right)$ is the hypergeometric series and $\mathbf{1}_n$ is a row vector of length n containing ones only.

For sufficiently large q the hypergeometric series approaches 1, which makes a truncation possible. It can be shown that the number of required terms for the sum increases with N_r and β. Although it can be seen from (19) that the detection probability is bounded between 0 and 1, it is not completely clear that a larger non-centrality parameter L (i.e., a higher SNR) leads to an improved detection performance. The latter reasoning may be explained as follows: Since with increasing L the maximum of $\frac{L^q}{2^q q!}$ shifts to larger values of q and since the hypergeometric series increases with q as well, a higher SNR results in an increased sum of the infinite series. As a consequence, a higher SNR leads to an improved detection performance.

VI. Detection Probability for Strong Signals

If the desired signal is strong[2], both the main lobe and the side lobes exceed the noise floor after correlation. In addition to that, cross-correlations with orthogonal signals may add to the side lobes of the desired signals, increasing the expected value of the second largest peak even further. In this case, both the largest and the second largest peak are assumed to follow a non-central χ^2-distribution but with different non-centrality parameters. This assumption overestimates the value of the second largest peak and leads to a lower bound on the detection probability [11].

The computation of the ratio between a non-central χ^2-distribution and the maximum of N_r samples following another non-central χ^2-distribution is quite difficult. It would be easier to add a scaled version of the correlation main lobe to the noise floor, so that the detection probability becomes

$$P_d(\beta) = \mathrm{P}\left(\frac{Y}{X_{(N_\mathrm{r})} + \alpha Y} > \beta\right) = \mathrm{P}\left(X_{(N_\mathrm{r})} < Y \frac{1-\alpha\beta}{\beta}\right) \tag{20}$$

where α is the scaling factor. This way it is assumed that the second largest peak of the decision metric is the combination of the largest of N_r noise samples and a scaled version of the correlation main lobe. The RV Y in (20) representing the main lobe already includes a certain amount of noise, which is thus added to the existing noise floor. Given that the scaling factor α is small enough, this noise contribution can be neglected. Since compared to the derivation in Section V only the threshold changed, (19) can be adapted to obtain a lower bound on the detection probability:

$$\begin{aligned} P_d(\beta) &= e^{-\frac{L}{2}} \sum_{q=0}^{\infty} \left[\frac{L^q}{2^q q!} \right. \\ &\left. \times \, {}_{q+2}F_{q+1}\left([-N_\mathrm{r}, \frac{\beta}{1-\alpha\beta}\mathbf{1}_{q+1}]; \frac{\beta+1-\alpha\beta}{1-\alpha\beta}\mathbf{1}_{q+1}; 1\right) \right] \end{aligned} \tag{21}$$

VII. Simulations and Results

A series of simulations was performed to verify the analytic results. For this purpose, a set of satellite signals was generated. It was assumed that four satellites (PRN codes 1, 8, 15, and 21) were visible with a Doppler shift $\theta_D = 0$. The satellites were assumed to have arbitrary code phase shifts relative to each other. For PRN codes 8, 15, and 21

[2] If the signal is strong, the probability that the largest sample stems from the signal is high, i.e. $\mathrm{P}(Y > X_{(N_\mathrm{r})}) \approx 1$.

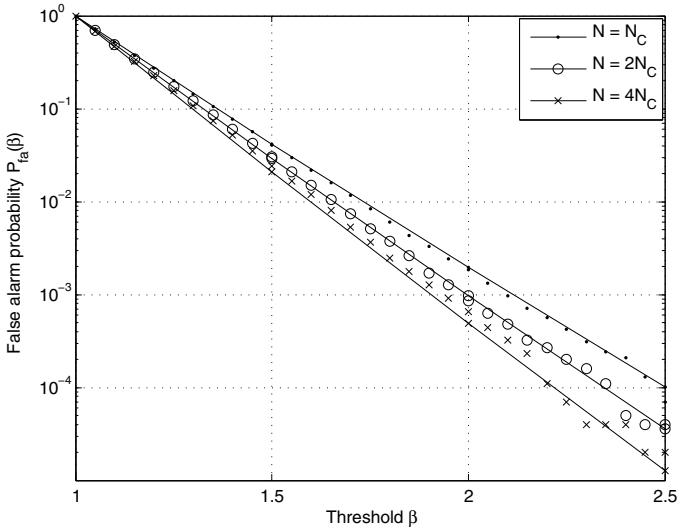

Fig. 2. False alarm probability $P_{fa}(\beta)$ for different FFT lengths N for analytic (lines) and simulated (markers) results. Simulations were done with one orthogonal code (PRN 1) at $\frac{C}{N_0} = 42$ dBHz.

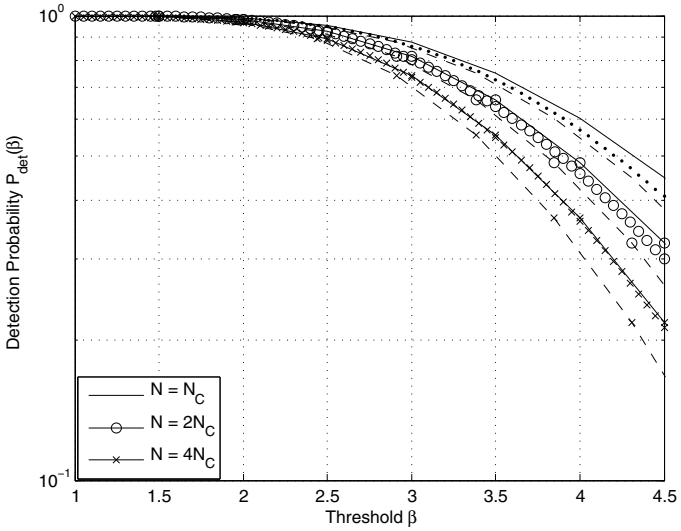

Fig. 3. Detection probability $P_d(\beta)$ for different thresholds β for $\frac{C}{N_0} = 45$ dBHz. Upper (solid) and lower (dashed) bounds are compared against simulations (markers).

$\frac{C}{N_0}$ was set to 12, 17, and 17 dBHz, while it was varied for the PRN code 1. The sampling rate was set to achieve FFT lengths $N = \{1, 2, 4\}N_C$ to ensure that consecutive samples of the decision metric are largely independent. For the sake of simplicity, the simulations only consider L1 C/A codes with $N_C = 1023$ and a code period of $T_{per} = 1$ ms.

The signals were correlated with PRN codes 1 and 5 for the detection and false alarm probabilities, respectively. A set of 10^5 correlations was performed for each value of N. For the lower bounds on the detection probability, the scaling factor α in Eq. 21 was set to 0.01 (-20 dB) to account for side lobes (-21 dB [5]) and cross-correlations with orthogonal codes.

A. False Alarm Probability

Fig. 2 shows the false alarm probability depending on the threshold β for different values of the FFT length N. It can be seen that for a given threshold β the false alarm probability decreases with an increasing value of N. This is understood from the fact that with an increasing number of samples N the ratio between the largest and the second largest sample decreases.

Comparing the analytic results with simulations, one can see that for sampling rates in the order of the chip rate indeed a good match can be achieved. It can be seen from Fig. 2 that by increasing the sampling rate the simulations match less and less the analytic results, which indicates that consecutive samples of the decision metric are not independent anymore.

B. Detection Probability

The detection probability $P_d(\beta)$ depending on the threshold β is depicted in Fig. 3 for different FFT lengths N. It can be seen that for large N the detection probability decreases, since with increasing N the expected value of the second largest peak increases while the value of the main lobe remains the same. Generally, the analytic bounds show a good match with the simulations, as long as the sampling rate is in the order of the chip rate.

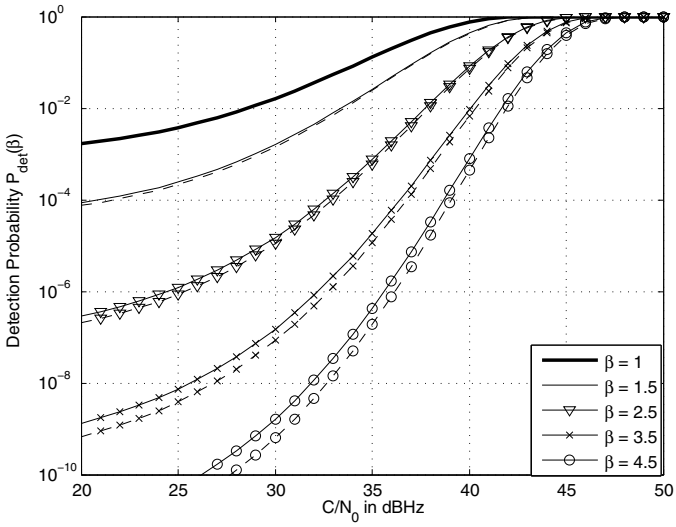

Fig. 4. Detection probability $P_d(\beta)$ for different values of $\frac{C}{N_0}$. The upper (solid) and lower (dashed) bounds on the detection probability are shown for an FFT size of $N = N_C = 1023$.

Fig. 4 shows the detection probability as a function of the signal power. Naturally, lower thresholds β and higher SNR lead to improved performance. Another interesting fact is revealed by looking at the thick solid line for $\beta = 1$: For low SNR, there is a significant probability that the largest peak stems from a noise sample, which makes a proper detection of the signal impossible.

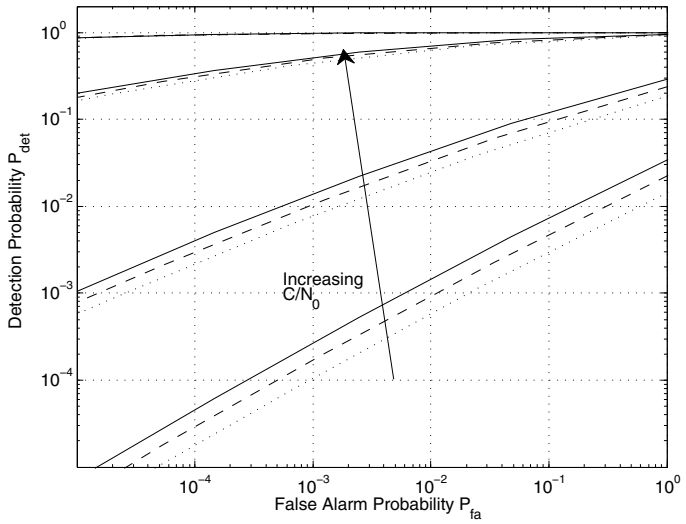

Fig. 5. Receiver operating characteristics. $N = N_C$ (solid), $N = 2N_C$ (dashed), and $N = 4N_C$ (dotted) were simulated. $\frac{C}{N_0}$ was varied within $\{32, 37, 42, 45\}$ dbHz.

C. Receiver Operating Characteristic (ROC)

Another interesting aspect can be seen by looking at Fig. 5 which shows the receiver operating characteristics (ROCs). It is shown that the performance of the receiver does not only depend on the SNR but also on the number of FFT samples. A higher number of FFT samples leads to a degraded performance in terms of detection, despite the fact that a longer FFT decreases the false alarm probability. This decrease in performance is less severe for high SNR values.

At the moment, the ROCs can not be directly compared to the results available in the literature about the acquisition of GPS signals, since either probabilities are derived for single cells [5] or for the whole two-dimensional search [11]. It is within the scope of future work to extend the analysis to the two-dimensional space by taking the search in the Doppler domain into account as well.

VIII. Conclusion

In this paper, the detection and false alarm probabilities for an FFT-based GPS acquisition method were derived. In this method, the complete circular correlation function for a certain Doppler shift is computed in a single step, and the satellite is assumed to be visible if the ratio between the largest and the second largest correlation value exceeds a certain threshold.

When employing such an acquisition method, the false alarm probability is independent of the SNR, which yields a constant false alarm rate for fixed thresholds. Furthermore, the probabilities depend on the length of the correlation function, which is proportional to the code period and the sampling rate. A set of simulations successfully verified the derived expressions.

Acknowledgments

This work was partially funded by the Austrian Research Promotion Agency under the project "SoftGNSS 2", project number 819682.

References

[1] D. M. Akos, P.-L. Normark, J.-T. Lee, and K. G. Gromov, "Low power global navigation satellite system (GNSS) signal detection and processing," in *ION GPS*, Sep. 2000, pp. 784–791.

[2] J. Jung, "Implementation of correlation power peak ratio based signal detection method," in *ION GNSS*, Sep. 2004, pp. 486–490.

[3] ——, "Receiver having a ratio-based signal acquisition method," U.S. Patent 7,161,977, Jan., 2007.

[4] K. Borre, D. M. Akos, N. Bertelsen, P. Rinder, and S. H. Jensen, *A Software-Defined GPS and Galileo Receiver: A Single Frequency Approach*. Birkhäuser, 2007.

[5] E. D. Kaplan and C. J. Hegarty, Eds., *Understanding GPS: Principles and Applications*, 2nd ed. Artech House, 2006.

[6] A. Polydoros and C. Weber, "A unified approach to serial search spread-spectrum code acquisition–part I: General theory," *IEEE Transactions on Communications*, vol. 32, no. 5, pp. 542–549, May 1984.

[7] ——, "A unified approach to serial search spread-spectrum code acquisition–part II: A matched-filter receiver," *IEEE Transactions on Communications*, vol. 32, no. 5, pp. 550–560, May 1984.

[8] U. Cheng, W. J. Hurd, and J. I. Statman, "Spread-spectrum code acquisition in the presence of Doppler shift and data modulation," *IEEE Transactions on Communications*, vol. 38, no. 2, pp. 241–250, Feb. 1990.

[9] J. H. J. Iinatti, "On the threshold setting principles in code acquisition of DS-SS signals," *IEEE Journal on Selected Areas in Communications*, vol. 18, no. 1, pp. 62–72, Jan. 2000.

[10] G. E. Corazza, "On the MAX/TC criterion for code acquisition and its application to DS-SSMA systems," *IEEE Transactions on Communications*, vol. 44, no. 9, pp. 1173–1182, Sep. 1996.

[11] D. Borio, L. Camoriano, and L. Lo Presti, "Impact of GPS acquisition strategy on decision probabilities," *IEEE Transactions on Aerospace and Electronic Systems*, vol. 44, no. 3, pp. 996–1011, Jul. 2008.

[12] D. Borio, C. O'Driscoll, and G. Lachapelle, "Coherent, non-coherent and differentially coherent combining techniques for the acquisition of new composite GNSS signals," *IEEE Transactions on Aerospace and Electronic Systems*, vol. 45, no. 3, pp. 1227–1240, Jul. 2009.

[13] A. Dempster, "Correlators for L2C: Some considerations," *InsideGNSS*, vol. October, pp. 32–37, Oct. 2006.

[14] S. U. Qaisar and A. Dempster, "Cross-correlation performance comparison of L1 & L2C GPS codes for weak signal acquisition," in *Int. Sym. on GPS/GNSS*, Nov. 2008.

[15] B. W. Parkinson and J. J. Spilker, *Global Positioning System: Theory and Applications, Volume I*. Progress in Astronautics and Aeronautics, 1996, vol. 163.

[16] J. A. Starzyk and Z. Zhu, "Averaging correlation for C/A code acquisition and tracking in frequency domain," in *IEEE Midwest Sym. on Circuits and Systems (MWSCAS)*, vol. 2, Aug. 2001, pp. 905–908.

[17] M. Fantino, A. Molino, and M. Nicola, "An acquisition strategy suitable for software GNSS receivers," in *European Navigation Conference - Global Navigation Satellite Systems (ENC-GNSS)*, May 2009.

[18] A. Papoulis and U. S. Pillai, *Probability, Random Variables and Stochastic Processes*, 4th ed. McGraw Hill, 2002.

[19] H. A. David and H. N. Nagaraja, *Order Statistics*, 3rd ed. John Wiley & Sons, 2003.

[20] M. Abramowitz and I. A. Stegun, Eds., *Handbook of Mathematical Functions with Formulas, Graphs, and Mathematical Tables*, 9th ed. Dover Publications, 1972.